# Spin-polarized electron tunneling through an aluminum particle in a noncollinear magnetic field

F. T. Birk, C. E. Malec, and D. Davidović
*School of Physics, Georgia Institute of Technology, Atlanta, Georgia 30332, USA*
(Received 8 April 2009; revised manuscript received 29 May 2009; published 22 June 2009)

We present measurements of spin-polarized electron tunneling through a nanometer-scale Al particle in contact with two ferromagnets as a function of the direction of the applied magnetic field at 4.2 K. We find that if the magnetizations of the ferromagnets are aligned parallel, the tunnel current has a weak dependence on magnetic-field direction $I_{\uparrow\uparrow} \approx \text{const}$, while if the magnetizations of the ferromagnets are aligned antiparallel, the current has significant dependence on magnetic-field direction $I_{\uparrow\downarrow}(\alpha) \approx I_{\uparrow\uparrow,0} \sin^2(\alpha) + I_{\uparrow\downarrow,0} \cos^2(\alpha)$, where $\alpha$ is the angle between the magnetic field and the magnetizations. Those dependencies are in agreement with the model of spin accumulation by incoherent electron transport via Zeeman-split energy levels of the particle. They demonstrate that the electron spin in the particle at finite current accumulates along the direction of the magnetic field rather than the magnetization direction. In zero magnetic field, the spin-accumulation direction is set by the field of the environment making it possible to study inhomogeneous spin dephasing. A lower limit of 8 ns is found for the inhomogeneous spin-dephasing time.

DOI: 10.1103/PhysRevB.79.245425 PACS number(s): 73.21.La, 72.25.Hg, 72.25.Rb, 73.23.Hk

## I. INTRODUCTION

Studies of spin-polarized electron conduction in a noncollinear magnetic field are important for injection, detection, and coherent manipulation of spins in electronic devices. In normal metals, electron spins can be injected from external ferromagnetic leads by tunneling. It has been demonstrated that a magnetic field applied perpendicular to the magnetization direction causes precession of the spin injected into the normal metal.[1,2] In that effect, the spin of an electron injected from the ferromagnet exhibits precessional motion about the magnetic field while the electron diffuses through the normal metal.

In nanometer-scale metallic particles, spin-polarized electron transport is different from that in macroscopic samples.[3,4] One important difference is the effect of the spin-orbit interaction.[5] In macroscopic metallic samples, where the electron-in-a-box level spacing $\delta$ is negligibly small, the spin-orbit interaction causes the electron wave functions to have an uncertain spin. As a result, an electron spin injected into such a sample will exhibit decay with the characteristic time equal to the spin-orbit scattering time $\tau_{SO}$.

In Al particles with diameter smaller than about 10 nm, the level spacing $\delta/\hbar$ becomes larger than the spin-orbit scattering rate $1/\tau_{SO}$. In that case, the spin-orbit scattering is quenched and the electron wave functions have certain spin.[6–8] Thus, the regime where $\delta\tau_{SO}/\hbar > 1$ is known as the regime of weak spin-orbit scattering. The electron-spin direction in such a particle can decay only by some coupling to the environment.[5,9] Evidence of long spin-relaxation time in metallic particles has been seen in spin-injection experiments where a single or an array of particles is attached by tunnel contacts to two ferromagnets.[5,10,11]

The main question addressed in this paper is whether the spin injected into the particle by tunneling from a ferromagnet exhibits precessional motion about a perpendicular magnetic field. Just as the finite level spacing quenches spin-orbit scattering, the spin precession may also be quenched. The origin of that quenching will be examined in Sec. II.

In this paper we study spin-polarized current through a single aluminum particle as a function of the magnetic-field direction. This study was motivated by the measurements of the spin precession in large-scale metallic samples discussed above[1,2] and our initial goal was to observe similar spin precession in a metallic particle. As will be shown in this paper, our data indicate that the spin precession is quenched. The experimental signature of the spin precession would be equal magnitudes of the dependencies of the current versus perpendicular field in the parallel and the antiparallel magnetized states of the leads. Instead, we observe significant field dependence of the current through the particle in the antiparallel magnetized state and only a weak dependence in the parallel magnetized state. These observations are explained by the Zeeman splitting of energy levels, which causes the tunnel coupling between the levels and the ferromagnetic leads to depend on the field direction.

In Sec. II we discuss electron tunneling via the particle states in a noncollinear magnetic field. In Sec. III we discuss sample fabrication and characterization. In Sec. IV, we revisit the effect of the saturation of the spin-polarized current through the particle published in our prior work. A reader interested only in the effect of the noncollinear field should skip to Sec. V. Finally, Sec. VI discusses spin dephasing.

## II. QUENCHING OF ELECTRON SPIN PRECESSION IN A METALLIC PARTICLE

In this section we discuss electron tunneling from a ferromagnet into a normal-metal particle in a noncollinear magnetic field. First we consider the case where the magnetic field is perpendicular to the magnetization.

In order to understand the sample size effects on spin precession, we will discuss in detail its microscopic mechanisms in a macroscopic sample. Consider a ferromagnet in tunnel contact with a normal metal. In the ferromagnet, the electron-spin direction is set along the exchange field direction. Consider an electron at energy $E$ and spin up incident on the tunnel barrier from the ferromagnet. Because the en-

 

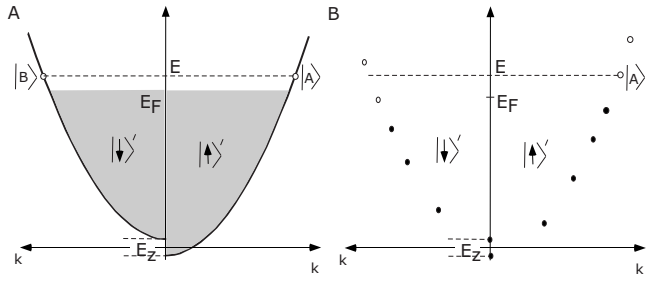


FIG. 1. (a) Spin degeneracy of the energy spectrum of a macroscopic metallic sample in a perpendicular field. (b) Absence of spin degeneracy in the energy spectrum of a metallic particle in a perpendicular field.

ergy spectrum in a large sample is continuous, the only restriction on $E$ in the normal metal is imposed by the Fermi-Dirac distribution. Figure 1(a) displays the single-electron energy spectrum of a macroscopic normal-metal sample in a perpendicular field.

As will be shown, for the spin-precession effect to take place after an electron tunnels elastically into the normal metal, it is necessary that the energy levels of the normal metal be spin degenerate. In particular, for any state $|A\rangle$ of the sample with spin pointing in the direction of the perpendicular field (say "spin up" or $|\uparrow\rangle'$) there should be a state $|B\rangle$ with opposite spin direction ("spin down" or $|\downarrow\rangle'$) and the same energy. The orbital wave functions of states $|A\rangle$ and $|B\rangle$ have slightly different wave vectors $k$ so that the difference in their kinetic energy is equal to $E_Z$, the Zeeman splitting in the perpendicular field. Because of the continuity of the spectrum, it will be possible to find such a pair of orbital wave functions at any $E_Z$ and $E$.

As a result, a spin-up electron can tunnel from the ferromagnet into the normal metal without changing its spin. There will exist a receiving state in the normal metal with spin up, which the electron can occupy after tunneling. In that state, the degenerate states $|A\rangle$ and $|B\rangle$ in Fig. 1 are coherently mixed to produce the spin-up state at the injection point. If the Zeeman splitting is close to zero, the receiving state would be $(|A\rangle+|B\rangle)/\sqrt{2}$.[12] In that case, spin is conserved in tunneling from the ferromagnet into the normal-metal sample and at finite bias voltage, the spin in the normal metal will accumulate along the magnetization direction consistent with experiments.[1,2]

To understand spin precession in a normal metal, we follow the trajectory of an electron after it is injected from the ferromagnet. The electron will follow a diffusive path through the metal with a diffusion constant $D=v_F l/3$. The correlated electron with opposite spin will follow a similar diffusive path, however, since their wave vectors differ by $E_Z/\hbar$, a phase difference develops, and the two electrons will only remain correlated over the correlation length $L_C=\sqrt{D\tau_C}$ where $\tau_C=\hbar/E_Z$.[13] On lengths less than this distance the spins remain correlated, and on lengths longer than this distance, the phase shift turns spin up into spin down resulting in spin precession. In this discussion we neglect spin-orbit scattering in the correlation region.

Going to nanometer-scale particles, this picture changes. If $\delta > E_Z$, all energy levels are nondegenerate as illustrated in Fig. 1(b). Nondegeneracy prevents coherent mixing between spin-up and spin-down states to produce a receiving state with spin up leading to the quenching of spin precession.

In some cases electron spin precession can occur in the particle. Recently, Braun *et al.*[14] calculated the current through a normal-metal particle in contact with ferromagnetic leads as a function of the magnetic field applied perpendicular to the magnetizations in the leads, which were collinear. Their model allows for the spin-up and spin-down states of the particle to mix coherently and considers the interplay between the Bloch equations and spin accumulation in the particle as a result of spin-dependent tunneling. The model predicts spin precession of the accumulated spin in the particle.

The condition of Braun's model is that the Zeeman splitting in the particle be weak, $E_Z/\hbar \sim \Gamma$, where $\Gamma$ is the electron tunnel rate between the particle and the ferromagnetic leads. In that regime the Zeeman-split states are broadened by the tunnel coupling. Additionally, the model is valid only at zero bias voltage, where sequential electron conduction can take place only if the background charge is $Q_0=(n+1/2)e$.

Our samples are usually measured at large bias voltage compared to $\delta/e$ and $E_Z/\hbar \gg \Gamma$, so in our samples the levels are not only nondegenerate but also nonoverlapping so there can be no coherent mixing between Zeeman-split levels. In that case, the contribution to electron current from different levels can be obtained using standard Coulomb blockade (CB) theory by summing the individual contributions of the levels incoherently, consistent with sequential electron tunneling.[15,16]

From now on we will assume that the magnetic field $\vec{B}$ can point in an arbitrary direction. We will consider a metallic particle in contact with two ferromagnets with collinear magnetizations. In the regime of well defined Zeeman levels of the particle, the tunnel rate between a level and the leads will depend on the direction of the magnetic field relative to the magnetizations.

In the ferromagnets, electrons move in an exchange field oriented along the $z$ axis so the spinors in the ferromagnets are $|\uparrow\rangle$ and $|\downarrow\rangle$. The tunnel density of states at the Fermi level of the ferromagnet will be characterized by the spin polarization $P$. In the particle, the Zeeman splitting in magnetic field $\vec{B}$ defines spinors $|\uparrow\rangle'$ and $|\downarrow\rangle'$ as shown in Fig. 2(a). The exchange field is negligible in the particle because our tunnel barriers are thick.

It will be assumed that the spin is conserved in the tunneling process across any of the two junctions. In a noncollinear magnetic field, we use a spinor transformation $|\uparrow\rangle'=\cos(\alpha/2)|\uparrow\rangle+\sin(\alpha/2)|\downarrow\rangle$ in the particle. If we consider the continuity of the wave function across the tunnel barrier, it will follow that the injection probability from the spin-up band into the state $|\uparrow\rangle'$ is proportional to $\cos^2(\alpha/2)$. Thus, the tunnel rate between level $|\uparrow\rangle'$ and the spin-up band in the ferromagnet can be written as $\Gamma^i(1+P)\cos^2(\alpha/2)$, where $i=\mathrm{L},\mathrm{R}$ for the left or right lead, respectively. The factor $(1+P)$ takes into account the spin-dependent tunnel density of states in the ferromagnetic leads. The injection from the spin-up band into $|\uparrow\rangle'$ will be accompanied by a spin-down reflection to satisfy spin conservation.

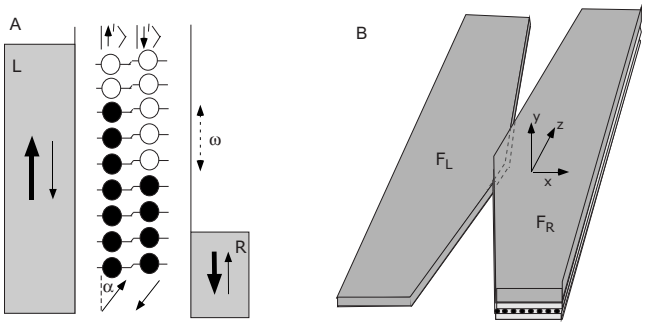


FIG. 2. (a) An excited state of the particle generated at finite bias voltage, fully relaxed with respect to spin-conserving transitions. Filled circles indicate occupied electron-in-a-box states. The spin expectation value is pointing along the magnetic field, which makes angle $\alpha$ with respect to the magnetizations. (b) Schematic of the sample.

In a noncollinear magnetic field, electron tunneling between the ferromagnetic leads and the particle will cause spin torque, which can be accompanied by precession of the spin accumulated in the particle.[17] In the analysis above, the reflection accompanied by spin reversal leads to that toque. The torque is proportional to the tunnel coupling $\Gamma$ between the leads and the particle.[17] Since the tunnel resistance is large in our samples the tunnel coupling will be very weak $(\Gamma/\delta \sim 10^{-5}-10^{-6})$, so the torque will be neglected in further analysis.

We obtain in a similar way the tunnel rate between $|\uparrow\rangle'$ and the spin-down band $\Gamma^i(1-P)\sin^2(\alpha/2)$. The total tunnel rate between level $|\uparrow\rangle'$ and lead $i$ is obtained by summing over the spin bands in the ferromagnet: $\Gamma^i_{|\uparrow\rangle'}(\alpha)=\Gamma^i(1+P)\cos^2(\alpha/2)+\Gamma^i(1-P)\sin^2(\alpha/2)=\Gamma^i[1+P\cos(\alpha)]$. Similarly, the total tunnel rate between level $|\downarrow\rangle'$ and lead $i$ is $\Gamma^i_{|\downarrow\rangle'}(\alpha)=\Gamma^i[1-P\cos(\alpha)]$. Thus, the overall effect of the field direction is to change the spin polarization in the leads from $P$ to an effective polarization $P\cos(\alpha)$.

At finite bias voltage, the spin-dependent tunnel rates lead to spin accumulation in the antiparallel magnetized configuration.[18–20] In general, the spin accumulation arises when one spin direction is preferentially injected into the particle from the source while the other spin direction is preferentially removed to the drain. Then, if the spin-relaxation time is longer than the electron dwell time on the particle, the excited particle states with one spin direction have a higher occupation probability compared to the states with opposite spin. As a result, the average spin polarization of the particle will be nonzero. Figure 2(a) illustrates spin accumulation.

Now we obtain the field-direction dependence of the current through the particle. In the parallel magnetized configuration, one spin direction is both preferentially injected and removed, so the average spin polarization of the particle is zero. In that case there will be no spin accumulation at any $\alpha$ because the effective polarization $P\cos(\alpha)$ is the same in both leads. In particular, if the preference to inject spins with one direction is reduced by $\cos(\alpha)$, then the preference to remove that spin will also be reduced by $\cos(\alpha)$, so the spin accumulation will remain zero and $I_{\uparrow\uparrow}$ versus $\alpha$ will be constant, $I_{\uparrow\uparrow}=I_{\uparrow\uparrow,0}$.

In the antiparallel magnetic state, sequential electron tunneling through the particle will cause spin accumulation, where the average number of occupied spin-up states is larger than the average number of occupied spin-down states. The average spin of the particle will point along the magnetic-field direction. By exchanging $P$ with $P\cos(\alpha)$ and using the spin-accumulation model appropriate for our samples,[9] we find

$$\Delta I = \Delta I_0 \cos^2(\alpha) = \Delta I_0 \frac{B_z^2}{B_\perp^2 + B_z^2}, \tag{1}$$

where $\Delta I=I_{\uparrow\uparrow}-I_{\uparrow\downarrow}$ is the difference in the current between the parallel and the antiparallel magnetic configuration in magnetic field $\vec{B}$ and $\Delta I_0=I_{\uparrow\uparrow,0}-I_{\uparrow\downarrow,0}$ is equal to the difference in the current between the parallel and the antiparallel magnetic configuration in zero magnetic field. Alternatively,

$$I_{\uparrow\downarrow} = I_{\uparrow\uparrow,0}\sin^2\alpha + I_{\uparrow\downarrow,0}\cos^2\alpha.$$

So, in the antiparallel magnetized state we expect that the current versus angle $\alpha$ will exhibit a minimum with a value equal to $I_{\uparrow\downarrow,0}$ at $\alpha=0$ and a value $I_{\uparrow\uparrow,0}$ at $\alpha=\pi/2$. This dependence reflects that the spin accumulation is reduced to zero when $\alpha$ varies from 0 to $\pi/2$. The current in Eq. (1) depends only on the field direction and not on the field magnitude.

This behavior should be contrasted with spin precession in macroscopic samples where spin precession would cause $I_{\uparrow\uparrow}$ versus perpendicular field to exhibit a maximum at $\alpha=0$. Additionally, in spin precession there would be a characteristic field scale given by the field at which the precession period is equal to the electron transit time. Experimentally, absence of field dependence in $I_{\uparrow\uparrow}$ combined with the field dependence in $I_{\uparrow\downarrow}$ following Eq. (1) should be the signature of the quenching of spin precession.

## III. SAMPLE FABRICATION AND CHARACTERIZATION

Our sample fabrication process has been described previously in Ref. 5. The schematic of the sample is displayed in Fig. 2(b). To summarize, we deposit two separate films elongated along the $z$ direction using the technique of shadow-mask deposition and electron-beam lithography with lift-off. The film on the left, $F_L$, is a 10-nm-thick layer of permalloy $(Ni_{0.8}Fe_{0.2})$. The film on the right is a multilayer consisting of four layers deposited in the following order from bottom to top: (1) 1.5-nm-thick layer of $Al_2O_3$, (2) 0.5-nm-thick layer of Al, (3) 1.5-nm-thick layer of $Al_2O_3$, and finally (4) 10-nm-thick layer of permalloy. The Al layer is so thin that the Al forms isolated particles.

The tunnel junction is located where the two films are overlapping. Many devices are made simultaneously with variable size of the overlap region, which varies from a large value to no overlap. As a function of the overlap size, the samples change from electrically conducting to insulating. The resistance of the samples versus overlap size exhibits a sharp conduction threshold. We then select the samples that are both conducting and near the conduction threshold, which virtually guarantees that the current between the leads

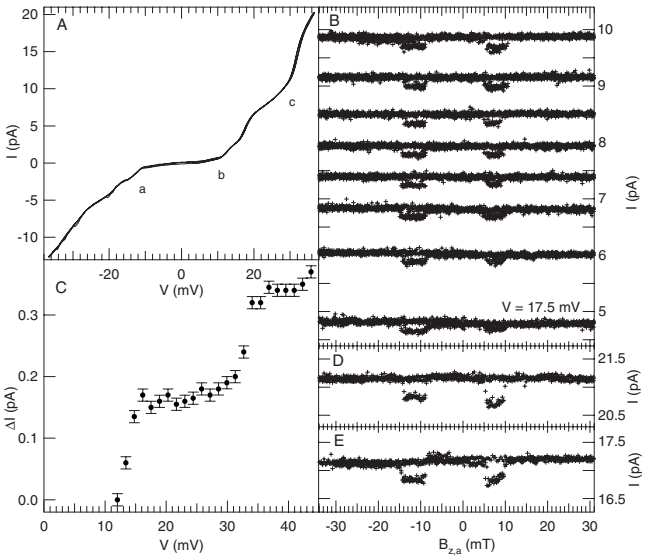


FIG. 3. (a) *I-V* curve at zero applied magnetic field. (b) *I* versus $B_{z,a}$, with increasing bias voltage. (c) $\Delta I = I_{\uparrow\uparrow} - I_{\uparrow\downarrow}$ versus *V*. [(d) and (e)] *I* versus $B_{z,a}$ at $V=35$ mV and $V=40$ mV, respectively. All data taken at $T=4.2$ K.

is flowing via a single particle.[5] The CB and, sometimes, spectroscopy of energy levels can be used to verify this tunneling condition. The arrangement of the leads is designed to stabilize the antiparallel magnetization configuration.

Typical particle parameters are $D \approx 5$ nm for the diameter and $\delta \sim 1$ meV for the level spacing. The $Al_2O_3$ thickness was chosen so that the tunnel resistance is high ($R \sim G\Omega$). In that case the tunnel rate is $\sim R_Q/R \cdot \delta/h \sim 1$ MHz, where $R_Q = h/e^2$. As discussed in previous papers,[5,9] the rate of the particle internal-relaxation transitions with spin flip, involving an energy difference $\delta$, is comparable to megahertz. The similarity between that spin-flip rate and the tunnel rate made it possible to explore the energy dependence of the spin-flip rate by transport measurements.[5,9]

The spin-conserving energy relaxation rate in the particle is much faster than the spin-relaxation rate. The spin-conserving energy relaxation occurs primarily through phonon emission and it is mediated by the electron-phonon interaction.[21] Theoretical estimate in Ref. 21 leads to the spin-conserving energy relaxation rate with energy difference $\delta$ of ~GHz, in agreement with that observed experimentally.[21,22]

So in our regime, at a bias voltage above the CB-threshold voltage, the particle is fully relaxed with respect to spin-conserving transitions. The particle can still remain in an excited state at time scales of $1/\Gamma$ provided that the excited states relax only by a spin-flip transition. One such excited state is displayed in Fig. 2(a). The spin-polarized excited states such as the one in Fig. 2(a) are responsible for spin accumulation and spin-polarized current.[9] Detailed discussion of the various internal transitions in the particle are available in Ref. 9.

Figure 3(a) displays the *I-V* curve of one device at 4.2 K, which exhibits CB. In addition to the conduction thresholds indicated by the letters a and b, there are thresholds at higher bias voltages where the slope of the *I-V* curve increases sharply, as indicated by the letter c at positive voltage. At the threshold voltages, additional charged states of the particle become energetically available for tunneling, consistent with CB.[15,23]

## IV. BIAS VOLTAGE AND SATURATION OF THE SPIN-POLARIZED CURRENT

In this section we discuss the spin-valve effect in sequential electron tunneling through the particle. We revisit the saturation of the spin-polarized current with bias voltage discussed in our prior work[5,9] and present additional data to confirm our prior observation as well as our interpretation. The discussion is placed within the context of the studies of magnetoresistance oscillations (MRO) in the single-electron charging regime,[24,25] emphasizing the difference between our saturation effect and the MRO. A reader primarily interested in the effect of noncollinear magnetic field should skip to Sec. V.

Current versus parallel applied field $B_{z,a}$ is displayed in Fig. 3(b). There are eight dependencies shown, each obtained at a different bias voltage. The bias voltage varies by 1.4 mV between successive dependencies. At each bias voltage, the field sweeps four times in the positive and negative field directions.

The dependencies signal the spin-valve effect. There are two pairs of magnetic transitions, one for each sweep direction. In a magnetic transition, the magnetic configuration switches between parallel and antiparallel, resulting in the current change $\Delta I = I_{\uparrow\uparrow} - I_{\uparrow\downarrow}$. Evidently the magnetic transitions are very reproducible at different bias voltages and with repeating scans.

In Fig. 3(b), $\Delta I \approx 0.17$ pA is nearly independent of *V* in the voltage interval between 17.5 and 27.3 mV. $\Delta I$ versus *V* over a broader voltage range is shown explicitly in Fig. 3(c). From $V=0$ to $V=32$ mV, $\Delta I$ displays saturation. We also measure the spin-valve signals at negative bias voltage and find the same behavior in $\Delta I$ versus *V* with the same magnitude of $\Delta I$.

By comparison, in ideal single magnetic tunnel junctions, $\Delta I$ would be linear with bias voltage within the range shown in Fig. 3(b). For that reason, single tunnel junctions are normally characterized by the tunnel magnetoresistance, TMR $= \Delta I / I_{\uparrow\uparrow}$, which is independent of *V* in ideal junctions.[26]

The saturation of $\Delta I$ versus *V* has been reported in our previous work,[5,9] where we show that the saturation occurs within the first few discrete energy levels available for tunneling above the CB-threshold voltage. The saturation was explained by a rapid decrease in spin-relaxation time $T_1$ versus energy difference $\omega$ in a spin-flip transition.

The rate of these transitions $1/T_1(\omega)$ increases rapidly with $\omega$. At low bias voltage measured from the CB-threshold voltage, Fig. 2 shows that the range of excitation energies $\omega$ of the particle will be small because that range is proportional to the voltage. In that case, $1/T_1(\omega) < \Gamma$ for any $\omega$, so $\Delta I$ will be linear with $I_{\uparrow\uparrow}$ and TMR will be constant. As the voltage increases, the range of $\omega$ also increases and $\Delta I$ saturates when there is an $\omega$ for which $1/T_1(\omega) \sim \Gamma$. Self-consistent calculation of the saturation parameters can be

done using a model in Ref. 9 leading to an estimate of $T_1(\delta) \approx 1$ $\mu$s.

$\Delta I$ versus $V$ in Fig. 3(c) exhibits another increase at $V \approx 32$ mV. The dependencies $I$ versus $B_z$ at $V > 32$ mV are shown in Figs. 3(d) and 3(e). $\Delta I$ in these figures is approximately two times larger than $\Delta I$ in Fig. 3(b). The data in Figs. 3(b)–3(e) are observations of a stepwise increase in the spin-polarized current with bias voltage through a metallic particle.

The increase in $\Delta I$ occurs at the conduction threshold voltage c in Fig. 3(a). At that voltage, an additional charged state becomes energetically available for electron tunneling and starts to contribute significantly to electron transport. So, adding a new charged state also adds a new channel for spin-polarized transport.

This second step observed in $\Delta I$ is explained as follows. At the threshold where the additional charged state becomes energetically available, there is insufficient energy to generate internally excited states in the particle, since the chemical potential in the source is equal to the charging energy for this additional charged state. Therefore, the particle in the additional charged state must be in the ground state. If the voltage is slightly larger than the threshold voltage, then the internal excitation energy $\omega$ will also be small for this new available state and the condition $1/T_1(\omega) < \Gamma$ will be satisfied again leading to spin accumulation.

One alternative explanation of the saturation effect in $\Delta I$ would be that it is caused by the magnetocoulomb effect.[3,27] In this effect, magnetization switching causes a shift in the background charge $\Delta Q_0$ of the particle. A $Q_0$ shift would shift the $I$-$V$ curve along the $V$ direction, which would cause $\Delta I$ versus $V$ to exhibit saturation, in qualitative agreement with our observations. But the magnetocoulomb effect has been ruled out as an explanation in our prior work[5] by measuring the spin-valve effect in the regime of resolved discrete energy levels. In particular, spin-valve effect was measured at voltages where the current was not sensitive to small $Q_0$ shifts.

As an additional assurance, we estimate the magnetocoulomb $Q_0$ shift in our sample and show that it should be negligible. From Ref. 3, we estimate $|\Delta Q_0/e| \sim PE_Z/E_C \sim 10^{-5}$, where $E_Z$ is the Zeeman energy at the coercive field ($\sim 10$ mT) and $E_C$ is the charging energy ($\sim 10$ meV). This $Q_0$ shift is very small because of the large charging energy. It would cause a shift in the current of about 0.1 fA while the measured value is $\Delta I = 0.17$ pA. So the contribution to $\Delta I$ from the magnetocoulomb effect can be neglected.

Another explanation of the saturation and the stepwise increase in $\Delta I$ versus bias voltage would be that it is caused by the MRO in ferromagnetic single-electron transistors.[24,25] If both the particle and the leads are ferromagnetic, then magnetoresistance oscillations arise from a combination of two effects: nonlinearity of the $I$-$V$ curve in the CB and the spin-dependent tunnel resistance. The nonlinearity depends on the tunnel resistances since they vary between the parallel and antiparallel magnetization configurations. The magnetoresistance will then exhibit oscillations with bias voltage in the range where the $I$-$V$ curve is nonlinear.

It has been predicted that MRO can also take place in a normal-metal particle in tunnel contact with two ferromagnetic leads, under the condition that the spin accumulation in the normal-metal particle is present.[18,28–33] In MRO with long spin-relaxation time, magnetoresistance remains within the same order of magnitude over a range of voltages involving several steps of the Coulomb staircase.[30] In our samples, the saturation of the spin-polarized current occurs within the first few discrete energy levels available for tunneling above the CB-threshold voltage.[5] At bias voltages above the saturation voltage, the TMR decreases as $1/V$. Moreover, TMR in our samples becomes strongly suppressed within the first step of the Coulomb staircase, in contrast to the MRO effect with long spin-relaxation time where TMR remains within the same order of magnitude. So, the saturation of the spin-polarized current observed in our samples cannot be explained by the MRO effects without taking into account the energy dependence of the spin-relaxation time.

Our samples have generally strong asymmetry of the tunnel junction resistance.[5,9] In that case, for a typical sample the $I$-$V$ curve above the CB-threshold voltage is linear at one sign of the bias voltage. We observe the saturation of $\Delta I$ with $V$ at voltages where the $I$-$V$ curve is linear and where the MRO effect should be weak.

If the bias voltage is reversed and the $I$-$V$ curve is nonlinear, the MRO effect could affect our spin-valve signal. However, we find that even in the nonlinear regime, $\Delta I$ saturates rapidly with bias voltage. Since the MRO vary with the energy scale set by the charging energy and our saturation effect is characterized by the energy scale comparable to $\delta$,[5] this is a further indication that the MRO cannot explain our observations.

To conclude, the MRO may play a role in the spin-valve effect in our samples depending on the sign of the bias voltage, but the rapid saturation of the spin-polarized current with bias voltage cannot be explained by the MRO without taking into account the energy dependence of the spin-relaxation time, which has the strongest effect on the bias-voltage dependence of the spin-valve signal.

We are aware of only one experimental group that has studied the bias-voltage dependence of the spin-valve signal in a single normal-metal particle.[3,10] They did not observe any saturation of the spin-valve signal but they did observe MRO. The difference between the two experiments can be attributed to the differences in the tunnel rate compared to the spin-relaxation rate. Our samples are 2 to 3 orders of magnitude higher in resistance ($R$) than those in Refs. 3 and 10. In addition, our particle diameters are about twice as large as those in Refs. 3 and 10, which means that the level spacing is reduced by an order of magnitude in our particle. Overall the tunnel rate $\Gamma \sim \delta/R$ in our samples is 3 to 4 orders of magnitude smaller than those in Refs. 3 and 10. As explained in our prior work,[9] the saturation voltage, measured from the CB-threshold voltage, is proportional to $\sim \Gamma^{1/4}$. The difference of 4 orders in magnitude in $\Gamma$ would lead to roughly an order of magnitude difference in the saturation voltage, which can explain the difference in the bias-voltage dependence of the spin-valve effect observed by the two groups.

However, in Refs. 3 and 10, the particle is Au, which has much stronger intrinsic spin-orbit scattering than Al. The difference in spin-orbit scattering would diminish the effect

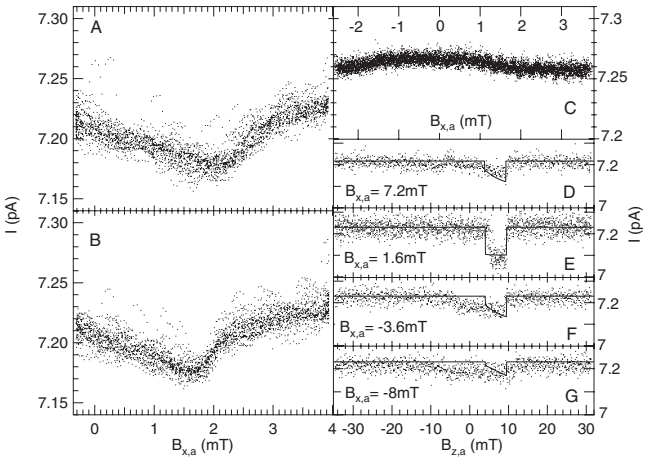


FIG. 4. [(a) and (b)] $I_{\uparrow\downarrow}$ versus $B_{x,a}$, for increasing and decreasing $B_{x,a}$, respectively, at $B_{y,a}=B_{z,a}=0$. (c) $I_{\uparrow\uparrow}$ versus $B_{x,a}$, at $B_{y,a}=B_{z,a}=0$. [(d)–(g)] Suppression of the spin-valve signal with perpendicular applied field. $T=4.2$ K in all figures.

caused by the difference in $\Gamma$. Thus, a more extensive study of the bias-voltage dependence of the spin-valve signal as a function of tunnel rate $\Gamma$ and material would be desirable.

## V. EFFECTS OF A NONCOLLINEAR MAGNETIC FIELD

In this section we investigate how a noncollinear magnetic field influences spin-polarized current through the particle. The magnetizations are set into the antiparallel configuration using the spin-valve signal. Figures 4(a) and 4(b) display current versus magnetic field applied along the $x$ axis, $B_{x,a}$, with the field being swept back and forth. The $x$ axis is indicated in Fig. 2(b).

The curve $I$ versus $B_{x,a}$ exhibits a minimum in the antiparallel configuration and weak dependence in the parallel configuration as can be seen in Figs. 4(a)–4(c). The minimum center is offset and its amplitude $\approx 0.05$ pA is smaller than $\Delta I=0.17$ pA measured in the spin-valve signal shown in Fig. 3. Comparing Figs. 4(a) and 4(b) the minimum is reversible with magnetic field, although there is a weak hysteresis of $\approx 0.2$ mT.

The spin-valve signal is suppressed in the presence of $B_{x,a}$ as shown in Figs. 4(d)–4(g). The strongest spin-valve signal [Fig. 4(e)] is measured around the minimum field in Figs. 4(a) and 4(b). For strong fields, Figs. 4(d), 4(f), and 4(g) show the magnetic transitions from parallel to the antiparallel magnetic state getting significantly weakened; as $B_{z,a}$ approaches the magnetic transition from antiparallel to the parallel state, there is now a gradual decrease in current. These transitions remain resolved but they get weakened proportionally to the magnitude of the perpendicular field indicating that the characteristic perpendicular field that weakens the spin-valve signal is much larger than the width of the minimum in Figs. 4(a) and 4(b).

At this point, we must rule out a possibility that the dependencies in Fig. 4 have been caused by rotation of the magnetizations in response to $B_{x,a}$ as it could explain the data

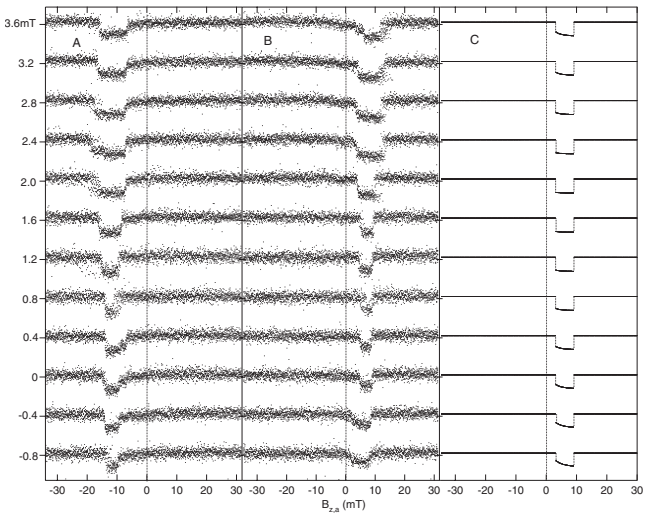


FIG. 5. [(a) and (b)] Spin-valve signals versus weak perpendicular field $B_{x,a}$, for decreasing and increasing $B_{z,a}$, respectively, at $T=4.2$ K. (c) Calculated spin-valve signal corresponding to Fig. 5(b).

so far presented. Starting from the antiparallel configuration, such a rotation would induce a flip into the parallel state leading to a minimum in $I$ versus $B_{x,a}$. Now from the parallel magnetic configuration, a rotation might not vary the angle between the magnetizations resulting in no dependence with perpendicular field.

Figure 5 displays a family of spin-valve signals measured at different fixed values of $B_{x,a}$ and taken within the field range of the minimum in Figs. 4(a) and 4(b). These curves are offset by 0.36 pA from each other for presentation purpose. The spin-valve effect is weakly affected by $B_{x,a}$, which demonstrates that the parallel and antiparallel configurations are stable in this field range.

We analyze the dependencies in Figs. 4 and 5 using Eq. (1), where $\vec{B}=\vec{B}_a+\vec{B}_l$. The fields $\vec{B}_a$ and $\vec{B}_l$ are the applied and the local field, respectively. $\vec{B}_l$ arises from the demagnetizing field generated by the leads, from the earth's magnetic field, and from the stray fields in the laboratory. Initially, we assume that the local field is static. In the section on electron dephasing we will consider a case when the local field has a time-dependent fluctuating component. $\Delta I_0$ in Eq. (1) is obtained as the maximum value of $I_{\uparrow\uparrow}-I_{\uparrow\downarrow}$ as a function of parallel and perpendicular applied fields in Fig. 5.

The amplitude, the full-width at half minimum, and the center of the curves in Figs. 4(a) and 4(b) should correspond to $\Delta I\frac{B_{z,l}^2}{B_{z,l}^2+B_{y,l}^2}$, $2\sqrt{B_{z,l}^2+B_{y,l}^2}$, and $-B_{x,l}$, respectively, from Eq. (1) which leads to $\vec{B}_l=(-1.8\ \text{mT}, \pm 0.63\ \text{mT}, \pm 0.41\ \text{mT})$.

Next, using this local field, Eq. (1), and the value of $\Delta I_0$ obtained as described above, we calculate the spin-valve signal using fixed coercive fields in the leads of 4 and 9 mT. The results of the calculation are indicated by the solid lines in Figs. 4(d)–4(g), showing good agreement with Eq. (1) without any fitting parameters.

The reason that the spin-valve signal in Fig. 5 is weakly affected by the perpendicular field, compared to Figs. 4(a) and 4(b) (where $B_{z,a}=0$), is that in the spin-valve signal, $B_{z,a}$

is large compared to $B_{x,a}$ in the antiparallel magnetic configuration. Figure 5(c) displays the spin-valve signal versus increasing $B_{x,a}$ calculated from Eq. (1) as explained above showing that the perpendicular field in Fig. 5 is weak to suppress the amplitude of the spin-valve signal. The calculation for decreasing $B_{x,a}$ leads to the same conclusion.

Since the dominant component of $\vec{B}_l$ is along $x$, this suggests that the local field is generated by a domain magnetized along the $x$ direction in the vicinity of the particle. Such a domain would explain the hysteresis and asymmetry in Figs. 4(a) and 4(b) if the domain wall moved in response to changing $B_{x,a}$. In that case the local field would not be completely independent of the applied field. Hysteresis of the domain-wall motion would lead to a hysteresis in $B_{x,l}$. The asymmetry of the minimum could also be attributed to the dependence of $B_{x,l}$ on $B_{x,a}$. But the hysteresis in $B_{x,l}$ is only 0.2 mT, which is about 10%. So in the lowest order of approximation, it can be assumed that the local field is constant in our applied field range.

To conclude, the spin-valve effect is affected by the perpendicular magnetic field in agreement with Eq. (1), which arises from the decomposition of the spinor in the particle in the basis of spinors in the ferromagnets. The current through the particle is weakly affected by the perpendicular field if the ferromagnets have parallel magnetization. In the antiparallel magnetization configuration, the perpendicular magnetic field increases the current through the particle from $I_{\uparrow\downarrow,0}$ to $I_{\uparrow\uparrow,0}$, as the magnetic-field vector is rotated from parallel to perpendicular direction relative to the magnetization. The absence of dependence in $I_{\uparrow\uparrow}$ versus $B_\perp$ and the agreement in $I_{\uparrow\downarrow}$ versus $B_\perp$ with Eq. (1) indicate that the spin precession in the particle is quenched and that spins in the particle accumulate along the direction of the magnetic field. This result should not be surprising because spin accumulation in the particle means that the average number of occupied "up" spinors must be larger than the average number of occupied "down" spinors in the particle, so the injected magnetization must point along the magnetic field.

## VI. EFFECT OF THE FLUCTUATING LOCAL MAGNETIC FIELD

The analysis of the results so far has neglected inhomogeneous spin dephasing from the local field in the particle. In a single metallic particle, temporal fluctuations of the local magnetic field can randomize the spin angle with respect to the $z$ axis.

One common source of that inhomogeneous spin dephasing in quantum dots is the hyperfine field of the nuclei.[34] An electron spin in an Al particle interacts with $N$ nuclear spins, where $N$ is the number of Al atoms in the particle. Those nuclear spins can be assumed random and uncorrelated in which case the total hyperfine field summed over the nuclei has a Gaussian distribution with standard deviation $\sim\sqrt{N}$. The sum has to be weighted by the magnitude square of the electron wave function at the nuclei, which is $\sim 1/V$ where $V$ is the particle volume. So the hyperfine field scales proportionally with $1/\sqrt{N}$; the larger the particle, the weaker the fluctuating hyperfine field.

In this discussion we will assume that the fluctuating field varies slowly compared to the tunneling rate and fast compared to the time that the current is measured ($\sim s$). In that case, the tunnel-in and tunnel-out rates between the particle and the leads follow the direction of the fluctuating field adiabatically. The measured current can be obtained by averaging over the Gaussian distribution of the fluctuating field

$$\Delta I(\vec{B}) = \Delta I_0 \int \frac{d^3\vec{B}'}{(\sigma\sqrt{2\pi})^3} \exp\left(-\frac{\vec{B}'^2}{2\sigma^2}\right) \frac{(B_z + B_z')^2}{(\vec{B}+\vec{B}')^2}. \quad (2)$$

In this equation, $\sigma$ is the standard deviation of a component of the fluctuating field assumed to be the same for $x$, $y$, and $z$ components. $\sigma$ is the measure of the fluctuating field. It sets the characteristic field scale for the angular dependence of the spin-polarized current.

We have calculated the integral in Eq. (2) numerically and obtained the magnetic-field dependence. Figure 6(a) displays $\Delta I/\Delta I_0$ versus perpendicular field $B_x/\sigma$ at different values of parallel field, $B_z/\sigma = 0$, 1, 2, 4, 6, and 12 and for $B_y = 0$.

In zero parallel field ($B_z = 0$), the spin-valve signal is reduced by 1/3 compared to the spin-valve signal in absence of the fluctuating field. Although the fluctuating field randomizes the spin axis in the particle, the spin-valve effect is not reduced to zero. The reason is that the spin-valve signal is proportional to $\cos^2(\alpha)$, where $\alpha$ is defined by the direction of the fluctuating field and the average of $\cos^2(\alpha)$ over the space angle is 1/3. The half-width at half maximum (HWHM) of the dependence at $B_z = 0$ is $2.04\sigma$, the same as that in the Gaussian distribution of the fluctuating field magnitude $\sqrt{B_x'^2 + B_y'^2 + B_z'^2}$[HWHM $= \sigma\sqrt{6\ln(2)}$].

A parallel magnetic field reduces the effect of the fluctuating field on the spin-valve signal and $\Delta I/\Delta I_0$ approaches 1 when $B_z \gg \sigma$. In a parallel field, the HWHM of $\Delta I/\Delta I_0$ versus $B_x$ is $\sqrt{(2.04\sigma)^2 + B_z^2}$.

The dependencies of the spin-valve signal on $B_x$ can also be changed by applying the field $B_y$ as shown in Fig. 6(b) where $B_y = 3\sigma$. As a function of increasing $B_y$, the magnitude of $\Delta I/\Delta I_0$ is suppressed and the width of $\Delta I/\Delta I_0$ versus $B_x$ is enhanced. Overall, HWHM $= \sqrt{(2.04\sigma)^2 + B_z^2 + B_y^2}$ for the dependence of the current on $B_x$.

With the data available thus far, there is insufficient information to determine both $\sigma$ and the static local field. Nevertheless, we can obtain a lower bound on $\sigma$ from the width of the dependence on perpendicular field, since HWHM $> 2.04\sigma$. Using the HWHM in Fig. 4 we obtain $\sigma < 0.37$ mT, or alternatively the rms fluctuating field magnitude $\sqrt{3}\sigma < 0.64$ mT. The inhomogeneous dephasing time is then given by the spin-precession time in the field of $\sqrt{3}\sigma$. Thus the inhomogeneous dephasing time is $T_2^\star > \hbar/(g\mu_B 0.64\ \text{mT}) \approx 8$ ns, which is enhanced compared to that in mesoscopic Al strips[2] and it is slightly larger than that measured in GaAs quantum dots.[35]

## VII. CONCLUSION

In conclusion, spin-polarized current through an aluminum particle is very sensitive to the direction of the applied magnetic field when the magnetizations in the ferromagnetic

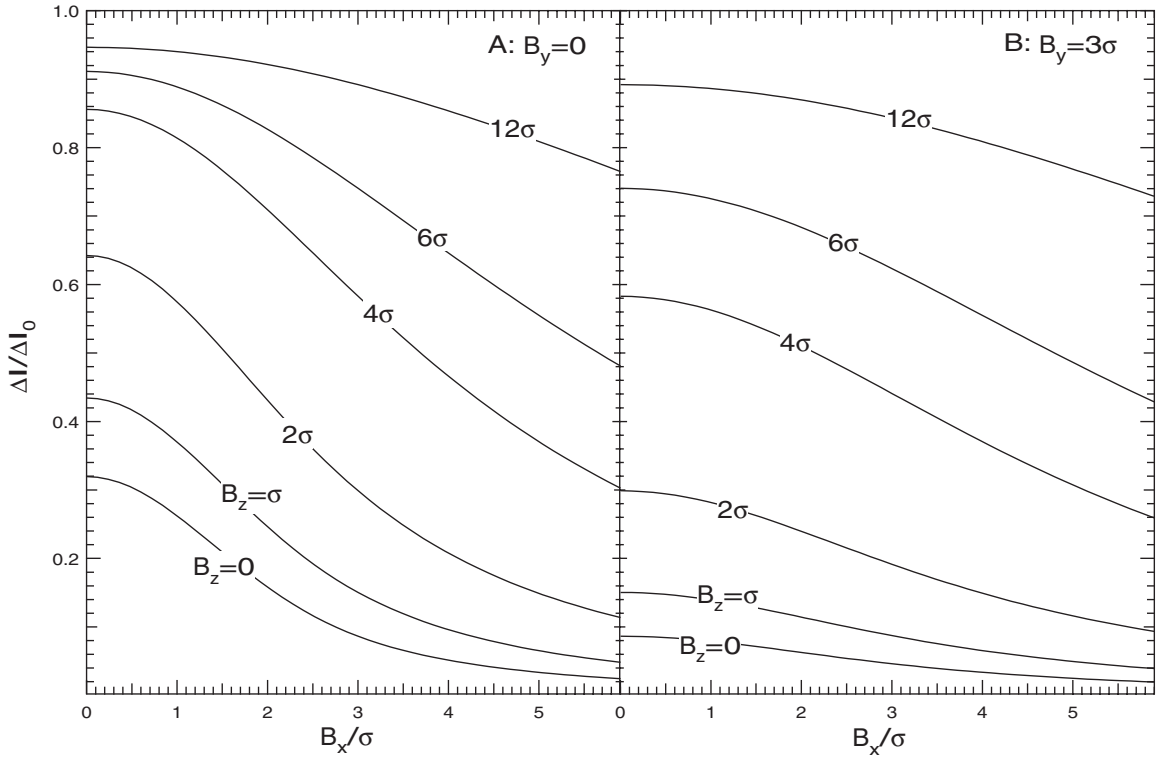


FIG. 6. [(a) and (b)] Normalized spin-valve signal ($I_{\uparrow\uparrow}-I_{\uparrow\downarrow}$) versus perpendicular field $B_x$, for $B_y=0$ and $B_y=3\sigma$, respectively. Different curves correspond to different magnetic fields parallel to the magnetization ($B_z$).

leads are antiparallel. The current is weakly dependent on the magnetic-field direction when the magnetizations in the leads are parallel. The field dependence of the spin-valve effect is in quantitative agreement with the model based on the decomposition of the spinors in the particle in terms of the spinor basis of the ferromagnetic leads. These observations demonstrate that the perpendicular magnetic field does not induce spin precession in the particle, or in other words, that the precession is quenched. The quenching is explained by the absence of spin degeneracy in the particle in a perpendicular magnetic field. A lower bound for the inhomogeneous spin-dephasing time of 8 ns is obtained from the characteristic field for the dependence of the current on the field direction when the magnetizations are antiparallel. Finally, a side result is that as a function of bias voltage, a stepwise increase in spin-polarized current is observed when an additional charged state of the nanoparticle becomes conductive, confirming long spin-relaxation time of weakly excited states of the nanoparticle.

## ACKNOWLEDGMENTS

This research was supported by the DOE and David and Lucile Packard Foundation.

[1] M. Johnson and R. H. Silsbee, Phys. Rev. Lett. **55**, 1790 (1985).
[2] F. J. Jedema, A. T. Filip, and B. J. van Wees, Nature (London) **410**, 345 (2001).
[3] P. Seneor, A. Bernand-Mantel, and F. Petroff, J. Phys.: Condens. Matter **19**, 165222 (2007).
[4] J. Barnas and I. Weymann, J. Phys.: Condens. Matter **20**, 423202 (2008).
[5] Y. G. Wei, C. E. Malec, and D. Davidovic, Phys. Rev. B **76**, 195327 (2007).
[6] D. G. Salinas, S. Gueron, D. C. Ralph, C. T. Black, and M. Tinkham, Phys. Rev. B **60**, 6137 (1999).
[7] K. A. Matveev, L. I. Glazman, and A. I. Larkin, Phys. Rev. Lett. **85**, 2789 (2000).
[8] P. W. Brouwer, X. Waintal, and B. I. Halperin, Phys. Rev. Lett. **85**, 369 (2000).
[9] Y. G. Wei, C. E. Malec, and D. Davidovic, Phys. Rev. B **78**, 035435 (2008).
[10] A. Bernand-Mantel, P. Seneor, N. Lidgi, M. Munoz, V. Cros, S. Fusil, K. Bouzehouane, C. Deranlot, A. Vaures, F. Petroff, and A. Fert, Appl. Phys. Lett. **89**, 062502 (2006).
[11] S. Mitani, Y. Nogi, H. Wang, K. Yakushiji, F. Ernult, and K. Takanashi, Appl. Phys. Lett. **92**, 152509 (2008).
[12] More generally, in a perpendicular field one has to take into account differences in the orbital states, $|A\rangle=u_{k_A}(\vec{r})|\uparrow\rangle'$ and $|B\rangle=u_{k_B}(\vec{r})|\downarrow\rangle'$. Then the receiving state is $C_1|A\rangle+C_2|B\rangle$, where $C_1$ and $C_2$ are obtained from the condition that the receiving state be proportional to $|\uparrow\rangle'+|\downarrow\rangle'$ at $\vec{r}=\vec{r}_I$, where $\vec{r}_I$ is the injection point.

[13] B. L. Altshuler and A. G. Aronov, in *Electron-Electron Interactions in Disordered Systems*, edited by A. L. Efros and M. Pollak (Elsevier, Amsterdam, 1985).
[14] M. Braun, J. Konig, and J. Martinek, Europhys. Lett. **72**, 294 (2005).
[15] D. V. Averin and K. K. Likharev, in *Mesoscopic Phenomena in Solids*, edited by B. L. Altshuler, P. L. Lee, and R. A. Webb (Elsevier, Amsterdam, 1991), p. 169.
[16] E. Bonet, M. M. Deshmukh, and D. C. Ralph, Phys. Rev. B **65**, 045317 (2002).
[17] J. Konig and J. Martinek, Phys. Rev. Lett. **90**, 166602 (2003).
[18] A. Brataas, Y. V. Nazarov, J. Inoue, and G. E. W. Bauer, Phys. Rev. B **59**, 93 (1999).
[19] I. Weymann, J. Konig, J. Martinek, J. Barnas, and G. Schon, Phys. Rev. B **72**, 115334 (2005).
[20] M. Braun, J. Konig, and J. Martinek, Phys. Rev. B **70**, 195345 (2004).
[21] O. Agam, N. S. Wingreen, B. L. Altshuler, D. C. Ralph, and M. Tinkham, Phys. Rev. Lett. **78**, 1956 (1997).
[22] D. C. Ralph, C. T. Black, and M. Tinkham, Phys. Rev. Lett. **74**, 3241 (1995).
[23] We compare $dI/dV$ versus $V$ with theoretical curves (Ref. 15) to identify the single-particle samples, the criteria introduced in Ref. 22 and used in our prior work (Ref. 5). Additionally, the sample is thermally cycled between 4.2 and 300 K several times, each time resulting in a different $I$-$V$ curve at 4.2 K, because of the different background charge $Q_0$. Various voltage thresholds are traceable with thermal cycling consistent with different $Q_0$ in electron transport in a single particle.
[24] J. Barnas and A. Fert, Phys. Rev. Lett. **80**, 1058 (1998).
[25] K. Majumdar and S. Hershfield, Phys. Rev. B **57**, 11521 (1998).
[26] M. Julliere, Phys. Lett. A **54**, 225 (1975).
[27] S. J. van der Molen, N. Tombros, and B. J. van Wees, Phys. Rev. B **73**, 220406(R) (2006).
[28] A. N. Korotkov and V. I. Safarov, Phys. Rev. B **59**, 89 (1999).
[29] J. Barnas and A. Fert, J. Magn. Magn. Mater. **192**, 391 (1999).
[30] I. Weymann and J. Barnas, Phys. Status Solidi B **236**, 651 (2003).
[31] W. Kuo and C. D. Chen, Phys. Rev. B **65**, 104427 (2002).
[32] A. Brataas and X. H. Wang, Phys. Rev. B **64**, 104434 (2001).
[33] W. Wetzels, G. E. W. Bauer, and M. Grifoni, Phys. Rev. B **72**, 020407(R) (2005).
[34] A. V. Khaetskii, D. Loss, and L. Glazman, Phys. Rev. Lett. **88**, 186802 (2002).
[35] J. R. Petta, A. C. Johnson, J. M. Taylor, E. A. Laird, A. Yacoby, M. D. Lukin, C. M. Marcus, M. P. Hanson, and A. C. Gossard, Science **309**, 2180 (2005).